Hindawi Publishing Corporation
Journal of Nanomaterials
Volume 2012, Article ID 912903, 9 pages
doi:10.1155/2012/912903

Review Article

Doping Silicon Nanocrystals with Boron and Phosphorus

Xiaodong Pi

State Key Laboratory of Silicon Materials and Department of Materials Science and Engineering, Zhejiang University, Zhejiang, Hangzhou 310027, China

Correspondence should be addressed to Xiaodong Pi, xdpi@zju.edu.cn

Received 29 April 2012; Accepted 21 August 2012

Academic Editor: Naoki Fukata

The properties of silicon nanocrystals (Si NCs) that are usually a few nanometers in size can be exquisitely tuned by boron (B) and phosphorus (P) doping. Recent progress in the simulation of B- and P-doped Si NCs has led to improved explanation for B- and P-doping-induced changes in the optical properties of Si NCs. This is mainly enabled by comprehensive investigation on the locations of B and P in Si NCs and the electronic properties of B- and P-doped Si NCs. I remarks on the implications of newly gained insights on B- and P-doped Si NCs. Continuous research to advance the understanding of the doping of Si NCs with B and P is envisioned.

1. Introduction

The electronic, optical, and magnetic properties of semiconductor nanocrystals (NCs) can be accurately tuned by controlling their size, shape, surface chemistry, and composition [1–3]. This enables great freedom for the applications of semiconductor NCs in a variety of fields such as electronics, optoelectronics, photovoltaics, and bioimaging [4, 5]. Among all the means for the tuning of the properties of semiconductor NCs, doping that only slightly modifies the composition of semiconductor NCs has been the focus in the past few years [6–8]. It is believed that new technologies based on semiconductor NCs may ultimately depend on doping, analogous to the critical role of doping in traditional semiconductor technologies.

Among all kinds of semiconductor NCs, silicon (Si) NCs are very attractive given the abundance and nontoxicity of Si [9]. It is well known that boron (B) and phosphorus (P) are the most widely used *p*-type and *n*-type dopants for bulk Si, respectively [10]. This leads to the doping of Si NCs by routinely using B and P [11–26]. In fact, concerns about unintentionally incorporated B and P in Si NCs appeared shortly after the discovery of efficient room-temperature light emission from porous Si, in which Si NCs were present [27–29]. Porous Si was obtained by electrochemically etching B- or P-doped Si wafers. B or P might unavoidably remain in the resulting porous structures. In late 1990s, Fujii et al. [11, 12] initiated the experimental study on the intentional doping of Si NCs that were embedded in silicon oxide. In the past few years, theoretical calculations have been carried out to elucidate the mechanisms underlying the doping-induced changes of the properties of Si NCs [30–38]. Experimental work has also been extended to the doping of freestanding Si NCs [17, 18, 21, 25].

Since the technological importance of Si NCs largely originates from their efficient light emission at room temperature [9, 39, 40], the effect of B and P doping on the optical properties of Si NCs is clearly the central research topic. Fujii has devoted one review to this topic based on the related work published before 2009 [41]. The current review deals with the progress in the research on the B and P doping of Si NCs with a focus on improved theoretical understanding. We start with the study of dopant locations. The discussion on the electronic and optical properties of Si NCs then follows. In the end, remarks and outlook are provided for the study of the doping of Si NCs with B and P.

2. Dopant Locations

It is generally believed that B and P atoms substitute Si atoms in bulk Si. Both B and P introduce very shallow energy levels in the bandgap of bulk Si (0.044 eV above the valence band for B and 0.045 eV below the conduction band for P) [10]. This causes B and P to be efficiently

ionized by thermal energy at room temperature, providing free carriers (holes induced by B and electrons induced by P) for electrical conduction in bulk Si. Given the large-scale practice of doping bulk Si with B and P in microelectronics, it is supposed that Si NCs should also be doped with B and P to facilitate the electronic transport in Si-NC-based devices. When we move to the nanometer-sized regime, however, the doping is complicated by the enormous surface area of Si NCs. B and P atoms may not only substitute Si atoms inside Si NCs, but also reside at the NC surface [36, 37]. The variation of dopant locations should significantly affect the electrical activity of B and P. Although the doping of B and P essentially aims to tune the electrical properties of Si NCs, it turns out that the remarkable optical properties of Si NCs are severely impacted [11, 12, 16, 17]. The optical activity of B and P may also be closely related to dopant locations.

It is rather challenging to experimentally determine the dopant locations for Si NCs that are a few nanometers large. Therefore, theoretical calculations have been playing a critical role in this aspect. It was initially shown that dopants preferred the near-surface region of Si NCs [30, 32]. Chen et al. [36] and Pi et al. [37] have recently demonstrated that the most feasible locations of dopants are actually at the NC surface by considering a variety of bonding configurations of dopants both inside Si NCs and at the NC surface.

2.1. B Doping. Figure 1 shows the formation energy (E_f) of selected B-doped Si NCs that are ~2.2 nm in diameter [37]. For all the doped Si NCs with substitutional B inside, the stability of a doped Si NC increases when B moves from the NC center to the NC surface (6 → 5 → 4 (4′) → 3 (3′) → 2 (2′)). There are 20 B configurations at the NC surface with E_f smaller than that for B2′ (one type of B located at the subsurface). This indicates that B prefers residing at the surface of Si NCs. Because the value of E_f for a Si NC with $B_{B2p}H_2$ (B passivating a surface Si atom that is originally passivated by two H atoms and being passivated by two H atoms, refer to [37] for detailed description on the configurations of B) is the lowest (Figure 1), B is most likely incorporated at the NC surface in the configuration of $B_{B2p}H_2$. As NC synthesis conditions change (e.g., the doping level of B increases), doped Si NCs with larger E_f may be formed. This predicts that following the formation of $B_{B2p}H_2$, other configurations of B such as $B_{C1s}H_2$, $B_{A2p}H_2$, $B_{A1p}H_2$, $B_{B1p}H_2$, $B_{B1s}H$, BH(α), $B_{B2s}H$, BH(β), $B_{C1p}H_2$, $B_{C2s}H_2$, $B_{C2p}H_2$, B_{A1s}, B_{A2s}, $B_{A1p}H_3$, $B_{A1s}H$, $B_{A2p}H_3$, $B_{B1s}H_2$, $B_{C1p}H_3$, and $BH_2(\alpha)$ should appear in sequence. Among these configurations BH(α), BH(β), and $BH_2(\alpha)$ result from surface restructuring [37]. It is interesting that B in most of the 20 B configurations at the NC surface (from $B_{B2p}H_2$ to B_{A2s}) is three-coordinated. This agrees with Polisski et al.'s speculation regarding Si NCs present in porous Si [29].

Pi et al.'s previous oxidation-etching experiment implied that B might be predominantly doped inside Si NCs because after the removal of surface oxide of oxidized B-doped Si NCs by hydrofluoric acid etching the concentration of B increased [17]. Such a result is in contrast with the theoretical prediction. The increase of B concentration may be due to the incorporation of B at the new NC surface during

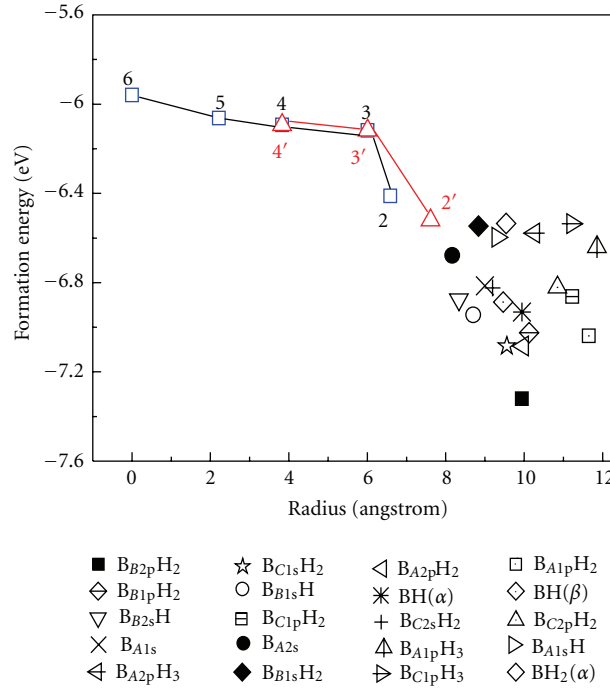

Figure 1: Formation energy of Si NCs doped with B in a variety of configurations. Among B configurations at the NC surface, only those with the formation energy of Si NCs smaller than that of a Si NC doped with B2′ are presented. They are $B_{B2p}H_2$, $B_{C1s}H_2$, $B_{A2p}H_2$, $B_{A1p}H_2$, $B_{B1p}H_2$, $B_{B1s}H$, BH(α), $B_{B2s}H$, BH(β), $B_{C1p}H_2$, $B_{C2s}H_2$, $B_{C2p}H_2$, B_{A1s}, B_{A2s}, $B_{A1p}H_3$, $B_{A1s}H$, $B_{A2p}H_3$, $B_{B1s}H_2$, $B_{C1p}H_3$, and $BH_2(\alpha)$. Internal substitutional B atoms from subsurface to the NC center (2 (2′) → 3 (3′) → 4 (4′) → 5 → 6) are all shown. (Reprinted from [37] copyright 2011 American Chemical Society.)

electrochemical etching. It is also possible that B at the NC surface is pushed toward the NC core in the oxidation-induced restructuring process. Ma et al. have recently calculated the formation energy of B in Si NCs with hydrogen deficiency at the NC surface [42]. They showed that B has a better chance to extend from the NC surface to the NC core when the NC surface is oxidized. Sugimoto et al. studied B-doped Si NCs derived from the HF etching of Si NC-embedding borosilicate glass [24]. They concluded that the surface of B-doped Si NCs was B-rich, consistent with theoretical prediction. It looks that this consistency is related to the guaranteed H passivation of Si NCs in Sugimoto's experiment.

2.2. P Doping. P is found to be most likely incorporated at the NC surface in the configurations of $P_{Ap}H_2$ (P passivating a surface Si atom that is originally passivated by one H atom and being passivated by two H atoms, refer to [36] for detailed description on the configurations of P) and P_{As} because the values of E_f for a Si NC with $P_{Ap}H_2$ and P_{As} are the lowest (Figure 2) [36]. At a given synthesis temperature, doped Si NCs with higher E_f may actually be formed when the doping level increases. We expect that following the formation of $P_{Ap}H_2$ and P_{As}, other configurations of P such as $P_{Bs}H$, $P_{Cp}H_2$, $P_{Bp}H_2$, and $P_{Cs}H_2$

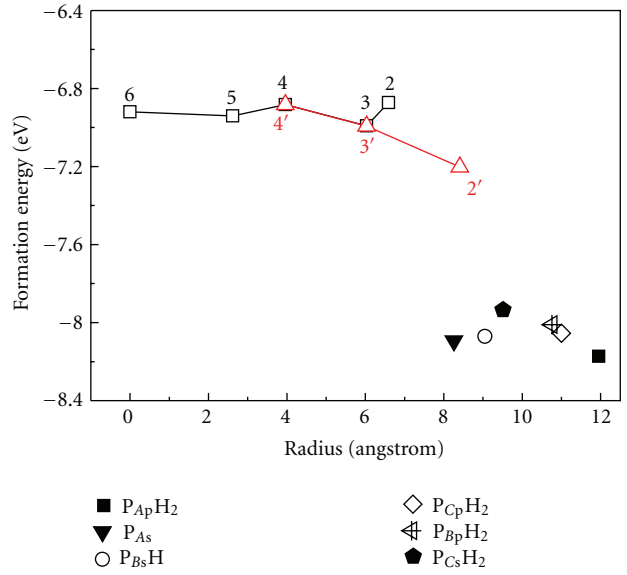

FIGURE 2: Formation energy of Si NCs doped with P in a variety of configurations. Among P configurations at the NC surface, only those with the formation energy of Si NCs smaller than that of a Si NC doped with P2′ are presented. They are $P_{Ap}H_2$, P_{As}, $P_{Bs}H$, $P_{Cp}H_2$, $P_{Bp}H_2$, and $P_{Cs}H_2$. Internal substitutional P atoms from subsurface to the NC center (2 (2′) → 3 (3′) → 4 (4′) → 5 → 6) are all shown. (Adapted from [36].)

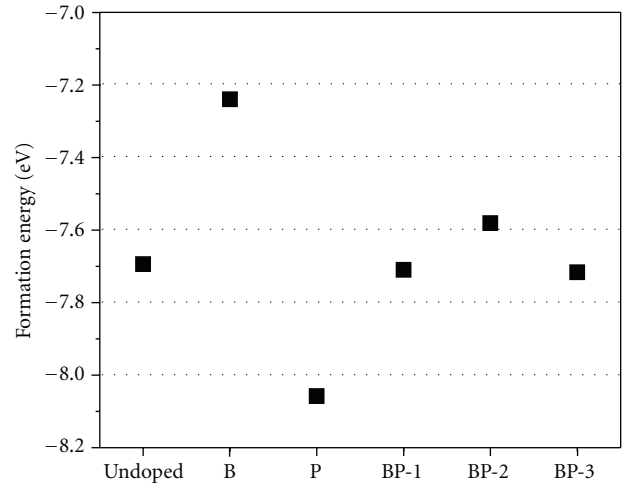

FIGURE 3: Formation energies of undoped, B-doped, P-doped, and lightly codoped Si NCs. (Reprinted from [38] copyright 2012 Springer.)

should appear in sequence as the doping level increases. P in all these configurations at the NC surface is three-coordinated, especially without dangling bonds. Therefore, the incorporation of P in these configurations effectively disables the formation of defects (dangling bonds) at the NC surface, suppressing defect-induced nonradiative events [43]. Recent experimental work has indicated that P is indeed preferentially incorporated at the surface of Si NCs [17, 21].

In addition, we should notice that the values of E_f for P-doped Si NCs are more than ~1 eV smaller than those for B-doped Si NCs (Figures 1 and 2). Such a difference in E_f may explain that the doping of P is more efficient than that of B for Si NCs that are a few nanometers large [17].

2.3. B and P Codoping. Since B and P are most likely located at the NC surface, we may assume that the incorporation of B and P inside the NC core only occurs during heavy doping. When we consider the codoping of Si NCs with B and P, B and P may be all located at the NC surface in the case of light doping [38]. Figure 3 shows the values of E_f for undoped, B-doped, P-doped, and lightly codoped Si NCs. B and P are in the configurations of $B_{B2p}H_2$ and P_{As}, respectively. For the three configurations in the codoping: BP-1 (P nearest neighbors B), BP-2 (P is 90° apart from B), and BP-3 (P and B are in crossing-diameter locations), the values of E_f for the lightly codoped NCs fall between those for the B- and P-doped NCs. The distance between B and P hardly affects the values of E_f for the lightly codoped NCs. Ossicini et al. previously investigated the codoping of Si NCs with B and P in the subsurface layer [31, 33]. They found that codoping was always energetically favored with respect to B or P doping. B and P tended to occupy the nearest neighboring sites in the subsurface layer. Clearly, these are in contrast to the case of light codoping. The current difference highlights the critical role of dopant location in the study of doped Si NCs. For light codoping B, and P atoms are at the NC surface, where there exists enough space for the steric relaxation of dopants. This leads to the negligible dependence of structural deformation on the dopant distance [31, 33].

3. Electronic and Optical Properties of Doped Si NCs

3.1. B Doping. Figure 4 shows energy-level diagrams for an undoped Si NC and doped Si NCs with E_f up to that of a Si NC doped with B6 (B in the NC center) [37]. The energy-level diagrams are arranged by the ascendant order of E_f for doped Si NCs. It is clear that the incorporation of all the B configurations in Figure 4 does not significantly modify the NC bandgap. B in doped Si NCs concerned in Figure 4(a) is all three-coordinated, consistent with the fact that B prefers sp^2-hybridation. The ground state of all the doped Si NCs in Figure 4(a) is singlet. We see that the majority of B configurations in Figure 4(a) introduce deep energy levels in the bandgap of Si NCs. These deep energy levels are induced by the localized empty $2p_z$ orbitals of B. For a Si NC with small or moderate quantum confinement, deep energy levels introduced by Si dangling bonds at the NC surface may quench the band-edge light emission from Si NCs [43]. In this study, the quantum confinement of 2.2 nm Si NCs is moderate. It is likely that deep energy levels introduced by B doping also quench the band-edge light emission from Si NCs. Therefore, the formation of a doped Si NC with E_f larger than that of a Si NC doped with $B_{A2p}H_2$ should be disabled to avoid the doping-induced quenching of band-edge light emission from Si NCs. By only considering nonphonon-assisted radiative band-edge

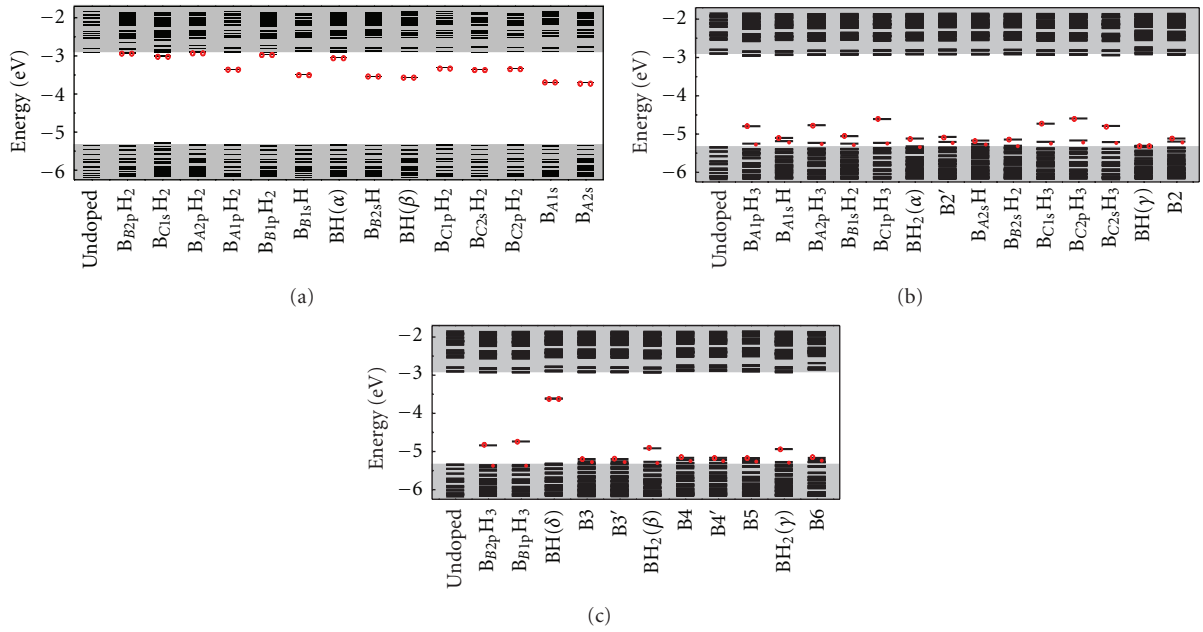

Figure 4: Energy-level diagram for an undoped or B-doped SiNC. B in the B configurations shown in (a) is all three-coordinated. Except for BH(γ and δ), B in the B configurations shown in (b) and (c) is all four-coordinated. Filled (empty) circles indicate that B-induced defect energy levels are occupied (unoccupied) by electrons. When B is four-coordinated, spin split occurs to the B-induced defect energy levels. (Reprinted from [37] copyright 2011 American Chemical Society.)

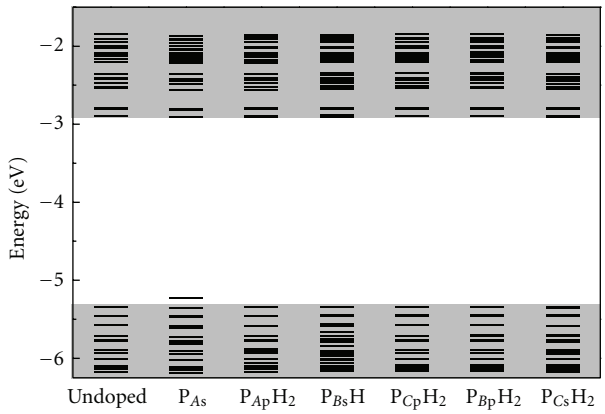

Figure 5: Energy-level diagram for an undoped or P-doped Si NC. P is in the configuration of P_{As}, $P_{Ap}H_2$, $P_{Bs}H$, $P_{Cp}H_2$, $P_{Bp}H_2$, and $P_{Cs}H_2$, which are all at the NC surface. (Reprinted from [36] copyright 2011 American Chemical Society.)

recombination (τ_R^{-1}) in Si NCs [36–38], we obtain that the values of τ_R^{-1} for an undoped Si NC and Si NCs doped with $B_{B2p}H_2$, $B_{C1s}H_2$, and $B_{A2p}H_2$ are 2.4×10^5, 6.7×10^6, 2.8×10^5, and 1.1×10^7 s^{-1}, respectively. This indicates that the doping of B may actually enhance the band-edge light emission from Si NCs if the formation of B configurations is limited to those with the three lowest values of E_f (i.e., $B_{B2p}H_2$, $B_{C1s}H_2$, and $B_{A2p}H_2$). In practice, it may be rather hard to exclusively dope Si NCs with $B_{B2p}H_2$, $B_{C1s}H_2$, and $B_{A2p}H_2$ given the required accurate experimental control. Besides the formation of these three B configurations, other B configurations may be routinely formed in experiments (please see their similar values of E_f in Figure 1), leading to the quenching of band-edge light emission from Si NCs.

Except for B in BH(γ) and BH(δ), B in the configurations concerned in Figures 4(b) and 4(c) is all four-coordinated. The originally empty $2p_z$ orbital of B forms a partial bond with a neighboring atom, which is also the case for B in bulk Si. This results in the doublet ground state. For all the four-coordinated B, B-induced energy levels are spin-split. The unoccupied energy levels of B are 0.2–0.8 eV away from the valence band. This means that all the four-coordinated B introduces deep energy levels, which may also lead to the quenching of the band-edge light emission from Si NCs. During the doping of Si NCs with B, only three-coordinated B configurations whose values of E_f for Si NCs are low likely appear. Electronic transitions from the valence band to the energy levels induced by these three-coordinated B are not in the infrared. This may explain the absence of the infrared absorption of B-doped Si NCs.

3.2. P Doping. P in the configurations of P_{As}, $P_{Ap}H_2$, $P_{Bs}H$, $P_{Cp}H_2$, $P_{Bp}H_2$, and $P_{Cs}H_2$ does not introduce any defect energy levels in the bandgap of Si NCs, as shown in Figure 5 [36]. This may be understood by considering the fact that the number of electrons in a Si NC doped with P in these configurations is even. The values of τ_R^{-1} in Si NCs with P in the configurations of P_{As}, $P_{Ap}H_2$, $P_{Bs}H$, $P_{Cp}H_2$, $P_{Bp}H_2$, and $P_{Cs}H_2$ are shown in Figure 6 [36]. It is seen that τ_R^{-1} is enhanced by a factor of at least 4, except for the only case of the formation of $P_{Bp}H_2$ at the NC surface. The enhancement of τ_R^{-1} together with the suppression of nonradiative events

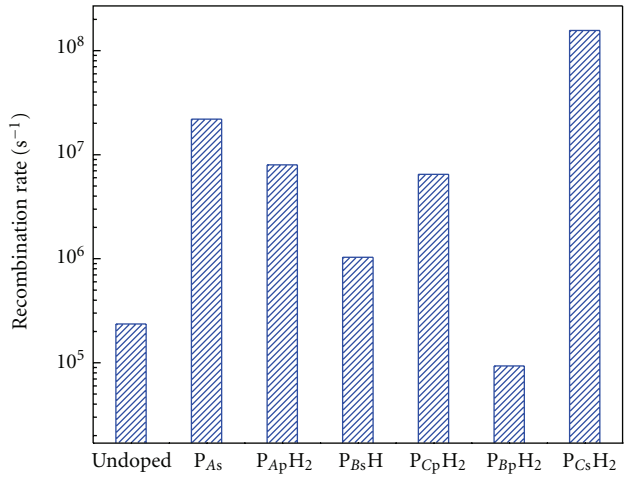

FIGURE 6: Rate of radiative band-edge recombination in an undoped or P-doped Si NC. P is in the configurations of P_{As}, $P_{Ap}H_2$, $P_{Bs}H$, $P_{Cp}H_2$, $P_{Bp}H_2$, and $P_{Cs}H_2$, which are all at the NC surface. (Reprinted from [36] copyright 2011 American Chemical Society.)

explains the increase in the PL efficiency of Si NCs as the doping level of P is low [12, 17, 22], since at a low doping level P is most likely incorporated at the surface of Si NCs in the configurations of P_{As}, $P_{Ap}H_2$, $P_{Bs}H$, $P_{Cp}H_2$, $P_{Bp}H_2$, and $P_{Cs}H_2$. It was shown that the lifetime of PL (τ_{PL}) from Si NCs also increased at a low doping level of P [12]. Given $\tau_{PL}^{-1} = \tau_R^{-1} + \tau_{NR}^{-1}$, τ_{NR}^{-1} should significantly decrease to counter the increase of τ_R^{-1}, ensuring a reduced τ_{PL}^{-1}. This means that the suppression of nonradiative events (i.e., the decrease of τ_{NR}^{-1}) plays a more important role in the enhancement of PL efficiency than the increase of τ_R^{-1}.

Figure 7 demonstrates that P in the configurations with higher E_f all introduces defect energy levels in the bandgap of Si NCs [36]. The introduction of defect energy levels is apparently related to the odd number of electrons in a Si NC doped with P. The spin splitting of P-doping induced defect states is caused by spin-orbit coupling. It can be concluded that P in all the configurations with high E_f results in the quenching of the band-edge light emission from Si NCs. This is consistent with experimental observation that the PL efficiency of Si NCs always decreases as the doping level of P is high [12, 17].

When the doping level of P is high, the number of doped P atoms per NC may be more than one. If we only consider combinations among the P configurations shown in Figure 7, a fair statistical analysis can be obtained to simulate the infrared absorption of P-doped Si NCs [36]. A variety of transitions involving P-induced defect energy levels may occur. The oscillator strengths of all the transitions that fall in the infrared region are illustrated in Figure 8. Data fitting gives $f \propto \lambda^{1.9}$ with a standard deviation of 0.4 in the power (f is oscillator strength and λ is wavelength). Since oscillator strength is proportional to absorption coefficient, the current result is basically similar to Mimura et al.'s observation on the variation of infrared absorption coefficient with wavelength for P-doped Si NCs [13].

3.3. B and P Codoping. For the light codoping that leads to the incorporation of dopants at the NC surface, a comparative study on the energy-level schemes of Si NCs is illustrated in Figure 9 [38]. It is seen that the incorporation of B slightly reduces the NC bandgap by lowering the lowest unoccupied molecular orbital (LUMO). The bandgaps of the P-doped Si NC and lightly codoped Si NCs are all reduced by ~0.15 eV. These reductions are mainly due to the P-induced increase of the highest occupied molecular orbital (HOMO). The energy levels of lightly codoped Si NCs are not significantly affected by the distance between dopants. This is due to the fact that P is mainly responsible for the reduction of the bandgap of Si NCs.

It has been found that light codoping causes the excitation energy and emission energy of Si NCs to redshift [38]. In most cases, the redshifts induced by light codoping is slightly larger than those induced by single-doping. For excitation energy, the largest redshift induced by light codoping is 0.04 eV more than that induced by single-doping (0.18 versus 0.14 eV). For emission energy, the largest redshift induced by light codoping is 0.02 eV more than that induced by single-doping (0.09 versus 0.07 eV). Since the largest redshift of 0.09 eV in emission energy induced by light codoping is actually small, light codoping should not be able to incur light emission with energy below the bandgap of bulk Si. This is in contrast to what happened to heavy codoping [15, 31, 33, 44]. If we assume that non-radiative recombination is negligible in all the Si NCs, we can state that the lightly codoped Si NCs more efficiently emit light than the undoped and B-doped Si NCs. The light emission efficiency of the lightly codoped Si NC with P nearest neighboring B is higher than that of the P-doped Si NC.

4. Remarks and Outlooks

The doping of bulk Si with B and P results in the internal incorporation of B and P into the substitutional sites of Si lattice. However, B and P prefer being located at the surface of Si NCs in terms of thermodynamics. It is well known that Si is a covalently bonded semiconductor, necessitating relatively high temperature for the formation of Si crystals. When Si NCs are formed in dielectric matrices, high temperatures between 1000 and 1200°C are routinely employed [11–16, 19, 20, 22–24, 26]. For Si NCs synthesized in plasma, selective nanoparticle heating causes the temperature of nanoparticles to exceed that of surrounding gas by several hundreds of kelvins [9, 17, 18, 21]. Therefore, it is reasonable to assume that thermal equilibrium is enabled by the relatively high temperatures of the Si-NC syntheses. As mentioned before, B and P thermodynamically prefer residing at the NC surface. Hence, the segregation of B and P at the NC surface may be expected. Clearly, the bonding of B (P) at the NC surface is different from that of B (P) in the substitutional sites of Si lattice. One can argue that Si NCs can not be successfully doped with B and P (especially when the doping level is low) although B and P are added to the synthesis system of Si NCs.

When B and P are at the NC surface, they do not produce very shallow energy levels. If the doping level is high, B and P may be incorporated into the substitutional sites

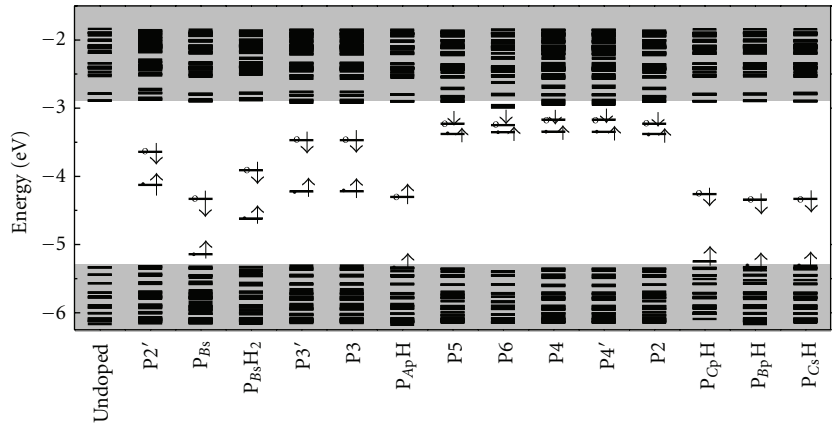

FIGURE 7: Energy-level diagram for an undoped or P-doped Si NC. P is in the configurations with high E_f. Filled (empty) circles indicate that P-induced defect energy levels are occupied (unoccupied) by electrons. Spin-up (spin-down) states of P-induced defect energy levels are indicated by up (down) arrows. (Reprinted from [36] copyright 2011 American Chemical Society).

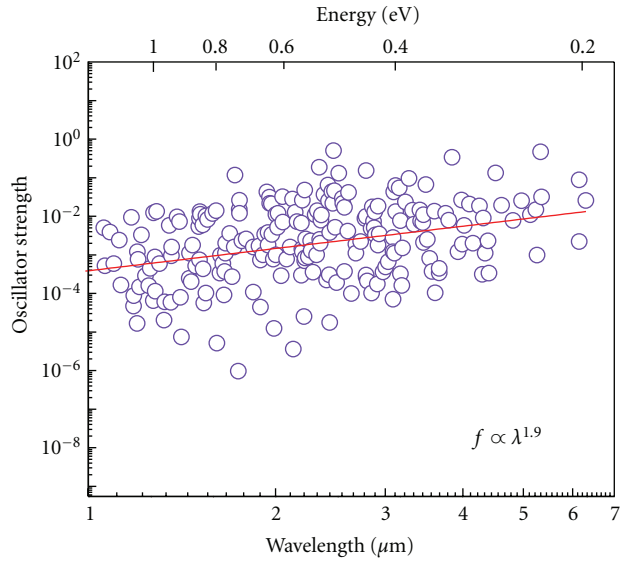

FIGURE 8: Oscillator strengths of the defect-related electronic transitions that fall in the infrared region. The defect energy levels are obtained by the optimization of a Si NC with two P atoms in the configurations considered in Figure 7. The red fitting line gives $f \propto \lambda^{1.9}$ with a standard deviation of 0.4 in the power (f is oscillator strength and λ is wavelength). (Reprinted from [36] copyright 2011 American Chemical Society.)

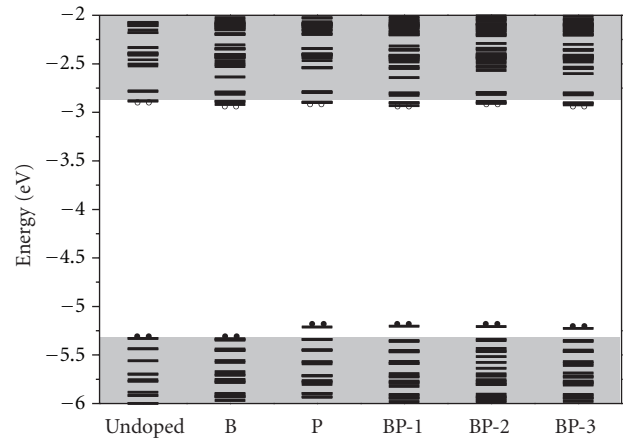

FIGURE 9: Energy-level diagrams for undoped, B-doped, P-doped, and lightly codoped Si NCs. Three configurations for the light codoping of B and P have been investigated: BP-1 (P nearest neighbors B), BP-2 (P is 90° apart from B), and BP-3 (P and B are in crossing-diameter locations). Filled (empty) circles indicate that the energy levels are occupied (unoccupied) by electrons. (Reprinted from [38] copyright 2012 Springer.)

inside Si NCs. But the substitutional B and P still do not produce very shallow energy levels. Therefore, B and P can not be ionized in Si NCs to produce carriers that are free inside the NCs. Given the fact that free carriers in the traditional sense remain physically confined inside Si NCs, researchers have opted to refer free carriers to those being able to move between Si NCs [30, 36, 45]. When this new concept of free carriers is adopted for Si NCs, the binding energy for dopants has been found to be pretty large. For example, the binding energy for P in the configurations concerned in Figure 5 is larger than 3.8 eV, while that for P in the configurations concerned in Figure 7 is larger than 2.0 eV. These large values of binding energy indicate that P produces no free carriers that can move between Si NCs at room temperature, consistent with the very low electrical conductivity of P-doped Si-NC films [18, 28]. Therefore, in terms of electrical activity, B and P are not dopants for Si NCs anymore. Nevertheless, for the sake of convenience we continue calling the incorporation of B and P into Si NCs doping.

It looks that the significance of doping Si NCs with B and P is mainly limited to the tuning of the optical properties of Si NCs up till now. All the theoretical investigation for the effect of doping on the optical properties of Si NCs has been based on the models of Si NCs fully passivated with H. However, oxide is routinely at the surface of Si NCs. Even if Si NCs are

originally passivated by H or organic ligands, they are at least partially oxidized after exposure to air [46–48]. Since oxide at the NC surface can make a difference for the properties of Si NCs [49–52], it will be more realistic to construct Si-NC models with oxide at the NC surface in the simulation of the doping of Si NCs.

It has been demonstrated that the doping of B may quench the band-edge light emission from Si NCs. As mentioned before, this was attributed to the B-induced nonradiative energy levels inside the bandgap of Si NCs [37]. However, Sugimoto et al. have recently proposed that the low-energy (~1.15 eV) light emission from B-doped Si NCs is due to the electronic transition involving B-induced energy levels inside the bandgap of Si NCs [24]. Whether the energy levels induced by B (especially B configurations concerned in Figure 4(a)) is radiative or not should be more carefully investigated to evaluate the correctness of Sugimoto et al.'s proposal. Sun et al. have also found pronounced low-energy (~0.95 eV) light emission from P-doped Si NCs [23]. They believed that the low-energy light emission originated from intrinsic defects in Si NCs. P doping may enhance the formation of these intrinsic defects. Future theoretical work should help to clarify the exact mechanism for the low-energy light emission from P-doped Si NCs.

The codoping of Si NC with B and P has been an added means to tune the properties of Si NCs. Since both B and P prefer being located at the NC surface, there should be B and P at the NC surface even in the case of heavy codoping. For better understanding on the sub-band light emission from heavily codoped Si NCs, more realistic Si-NC models in which B and P are both at the NC surface and inside the NC core should be employed. Fukuda et al. have recently demonstrated that codoped Si NCs may be very well dispersed in polar solvents such as methanol [53]. Such an interesting phenomenon was explained by the consideration of an electrical double layer at the surface of Si NCs. The electrical double layer consists of an inner P-rich shell and an outer B-rich shell. Given the high desirability of dispersible Si NCs without organic ligands at the NC surface in the preparation of Si ink [54, 55], doping may also play a critical role in the processing of printed Si electronics.

5. Conclusion

Progress in the understanding of B- and P-doping-induced changes in the electronic and optical properties of Si NCs has been made recently. This is achieved by carefully investigating the locations of B and P not only inside Si NCs but also at the surface of Si NCs. Both B and P are found to thermodynamically prefer residing at the NC surface. While doping levels are high, B and P may be incorporated inside Si NCs. Energy-level schemes for B- and P-doped Si NCs can be reasonably correlated to their optical absorption and emission. In the traditional sense of doping, B and P are not dopants for Si NCs that are a few nanometers large any more. On one hand, B and P may be only at the NC surface. On the other hand, neither internal B/P nor surface B/P can produce free carriers for Si NCs. Nevertheless, B and P can be called dopants for convenience. For better understanding of the properties of B- and P-doped Si NCs, more realistic models of Si NCs should be employed in the future. Further investigation needs to be carried out to clarify if recombination involving B- and P-induced energy levels is radiative or not. With the continuous progress in the doping-enabled tuning of the properties of Si NCs, there exist good opportunities for both experimental and theoretical research on doped Si NCs.

Acknowledgments

Shanghai Supercomputer Center is thanked for providing computation resources. This work was mainly supported by the National Natural Science Foundation of China (Grant no. 50902122). Partial support from the R&D Program of Ministry of Education of China (Grant no. 62501040202), the Innovation Team Project of Zhejiang Province (Grant no. 2009R50005), Scientific Research Foundation for Returned Scholars from the Ministry of Human Resources and Social Security of China (Grant no. 20100129), the 2011 Sino-French Xu Guangqi program, and the Major Scientific program of Zhejiang Province (Grant no. 2009C01024-2) is acknowledged.

References

[1] Y. Yin and A. P. Alivisatos, "Colloidal nanocrystal synthesis and the organic-inorganic interface," *Nature*, vol. 437, no. 7059, pp. 664–670, 2005.

[2] J. G. C. Veinot, "Synthesis, surface functionalization, and properties of freestanding silicon nanocrystals," *Chemical Communications*, no. 40, pp. 4160–4168, 2006.

[3] R. Beaulac, P. I. Archer, S. T. Ochsenbein, and D. R. Gamelin, "Mn^{2+}-doped CdSe quantum dots: new inorganic materials for spin-electronics and spin-photonics," *Advanced Functional Materials*, vol. 18, no. 24, pp. 3873–3891, 2008.

[4] D. V. Talapin, J. S. Lee, M. V. Kovalenko, and E. V. Shevchenko, "Prospects of colloidal nanocrystals for electronic and optoelectronic applications," *Chemical Reviews*, vol. 110, no. 1, pp. 389–458, 2010.

[5] N. O'Farrell, A. Houlton, and B. R. Horrocks, "Silicon nanoparticles: applications in cell biology and medicine," *International Journal of Nanomedicine*, vol. 1, no. 4, pp. 451–472, 2006.

[6] D. J. Norris, A. L. Efros, and S. C. Erwin, "Doped nanocrystals," *Science*, vol. 319, no. 5871, pp. 1776–1779, 2008.

[7] S. C. Erwin, L. Zu, M. I. Haftel, A. L. Efros, T. A. Kennedy, and D. J. Norris, "Doping semiconductor nanocrystals," *Nature*, vol. 436, no. 7047, pp. 91–94, 2005.

[8] D. Mocatta, G. Cohen, J. Schattner, O. Millo, E. Rabani, and U. Banin, "Heavily doped semiconductor nanocrystal quantum dots," *Science*, vol. 332, no. 6025, pp. 77–81, 2011.

[9] U. Kortshagen, "Nonthermal plasma synthesis of semiconductor nanocrystals," *Journal of Physics D*, vol. 42, no. 11, Article ID 113001, 2009.

[10] S. M. Sze and K. K. Ng, *Physics of Semiconductor Devices*, John Wiley & Sons, New York, NY, USA, 2006.

[11] M. Fujii, S. Hayashi, and K. Yamamoto, "Photoluminescence from B-doped Si nanocrystals," *Journal of Applied Physics*, vol. 83, no. 12, pp. 7953–7957, 1998.

[12] M. Fujii, A. Mimura, S. Hayashi, and K. Yamamoto, "Photoluminescence from Si nanocrystals dispersed in phosphosilicate glass thin films: improvement of photoluminescence efficiency," *Applied Physics Letters*, vol. 75, no. 2, pp. 184–186, 1999.

[13] A. Mimura, M. Fujii, S. Hayashi, D. Kovalev, and F. Koch, "Photoluminescence and free-electron absorption in heavily phosphorus-doped Si nanocrystals," *Physical Review B*, vol. 62, no. 19, pp. 12625–12627, 2000.

[14] M. Fujii, A. Mimura, S. Hayashi, Y. Yamamoto, and K. Murakami, "Hyperfine structure of the electron spin resonance of phosphorus-doped Si nanocrystals," *Physical Review Letters*, vol. 89, no. 20, Article ID 206805, 4 pages, 2002.

[15] M. Fujii, K. Toshikiyo, Y. Takase, Y. Yamaguchi, and S. Hayashi, "Below bulk-band-gap photoluminescence at room temperature from heavily P- and B-doped Si nanocrystals," *Journal of Applied Physics*, vol. 94, no. 3, pp. 1990–1995, 2003.

[16] M. Fujii, Y. Yamaguchi, Y. Takase, K. Ninomiya, and S. Hayashi, "Control of photoluminescence properties of Si nanocrystals by simultaneously doping n- and P-type impurities," *Applied Physics Letters*, vol. 85, no. 7, pp. 1158–1160, 2004.

[17] X. D. Pi, R. Gresback, R. W. Liptak, S. A. Campbell, and U. Kortshagen, "Doping efficiency, dopant location, and oxidation of Si nanocrystals," *Applied Physics Letters*, vol. 92, no. 12, Article ID 123102, 3 pages, 2008.

[18] A. R. Stegner, R. N. Pereira, K. Klein et al., "Electronic transport in phosphorus-doped silicon nanocrystal networks," *Physical Review Letters*, vol. 100, no. 2, Article ID 026803, 4 pages, 2008.

[19] X. J. Hao, E. C. Cho, C. Flynn et al., "Synthesis and characterization of boron-doped Si quantum dots for all-Si quantum dot tandem solar cells," *Solar Energy Materials and Solar Cells*, vol. 93, no. 2, pp. 273–279, 2009.

[20] K. Sato, N. Fukata, and K. Hirakuri, "Doping and characterization of boron atoms in nanocrystalline silicon particles," *Applied Physics Letters*, vol. 94, no. 16, Article ID 161902, 3 pages, 2009.

[21] A. R. Stegner, R. N. Pereira, R. Lechner et al., "Doping efficiency in freestanding silicon nanocrystals from the gas phase: phosphorus incorporation and defect-induced compensation," *Physical Review B*, vol. 80, no. 16, Article ID 165326, 10 pages, 2009.

[22] M. Perego, C. Bonafos, and M. Fanciulli, "Phosphorus doping of ultra-small silicon nanocrystals," *Nanotechnology*, vol. 21, no. 2, Article ID 025602, 2010.

[23] H. C. Sun, J. Xu, Y. Liu et al., "Subband light emission from phosphorous-doped amorphous Si/SiO_2 multilayers at room temperature," *Chinese Physics Letters*, vol. 28, no. 6, Article ID 067802, 2011.

[24] H. Sugimoto, M. Fujii, M. Fukuda, K. Imakita, and S. Hayashi, "Acceptor-related low-energy photoluminescence from boron-doped Si nanocrystals," *Journal of Applied Physics*, vol. 110, no. 6, Article ID 063528, 6 pages, 2011.

[25] R. K. Baldwin, J. Zou, K. A. Pettigrew, G. J. Yeagle, R. D. Britt, and S. M. Kauzlarich, "The preparation of a phosphorus doped silicon film from phosphorus containing silicon nanoparticles," *Chemical Communications*, vol. 6, no. 6, pp. 658–660, 2006.

[26] K. Imakita, M. Ito, M. Fujii, and S. Hayashi, "Nonlinear optical properties of phosphorous-doped Si nanocrystals embedded in phosphosilicate glass thin films," *Optics Express*, vol. 17, no. 9, pp. 7368–7376, 2009.

[27] G. Mauckner, W. Rebitzer, K. Thonke, and R. Sauer, "Quantum confinement effects in absorption and emission of freestanding porous silicon," *Solid State Communications*, vol. 91, no. 9, pp. 717–720, 1994.

[28] A. J. Simons, T. I. Cox, M. J. Uren, and P. D. J. Calcott, "The electrical properties of porous silicon produced from n^+ silicon substrates," *Thin Solid Films*, vol. 255, no. 1-2, pp. 12–15, 1995.

[29] G. Polisski, D. Kovalev, G. Dollinger, T. Sulima, and F. Koch, "Boron in mesoporous Si—where have all the carriers gone?" *Physica B*, vol. 273-274, pp. 951–954, 1999.

[30] G. Cantele, E. Degoli, E. Luppi et al., "First-principles study of n- and p-doped silicon nanoclusters," *Physical Review B*, vol. 72, no. 11, Article ID 113303, 4 pages, 2005.

[31] S. Ossicini, E. Degoli, F. Iori et al., "Simultaneously B- and P-doped silicon nanoclusters: formation energies and electronic properties," *Applied Physics Letters*, vol. 87, no. 17, Article ID 173120, 3 pages, 2005.

[32] T. L. Chan, M. L. Tiago, E. Kaxiras, and J. R. Chelikowsky, "Size limits on doping phosphorus into silicon nanocrystals," *Nano Letters*, vol. 8, no. 2, pp. 596–600, 2008.

[33] F. Iori, E. Degoli, R. Magri et al., "Engineering silicon nanocrystals: theoretical study of the effect of codoping with boron and phosphorus," *Physical Review B*, vol. 76, no. 8, Article ID 085302, 14 pages, 2007.

[34] Q. Xu, J. W. Luo, S. S. Li, J. B. Xia, J. Li, and S. H. Wei, "Chemical trends of defect formation in Si quantum dots: the case of group-III and group-V dopants," *Physical Review B*, vol. 75, no. 23, Article ID 235304, 6 pages, 2007.

[35] L. E. Ramos, E. Degoli, G. Cantele et al., "Optical absorption spectra of doped and codoped Si nanocrystallites," *Physical Review B*, vol. 78, no. 23, Article ID 235310, 11 pages, 2008.

[36] X. Chen, X. Pi, and D. Yang, "Critical role of dopant location for P-doped Si nanocrystals," *Journal of Physical Chemistry C*, vol. 115, no. 3, pp. 661–666, 2011.

[37] X. D. Pi, X. B. Chen, and D. Yang, "First-principles study of 2.2 nm silicon nanocrystals doped with boron," *Journal of Physical Chemistry C*, vol. 115, no. 20, pp. 9838–9843, 2011.

[38] Y. S. Ma, X. B. Chen, X. D. Pi, and D. Yang, "Lightly boron and phosphorus co-doped silicon nanocrystals," *Journal of Nanoparticle Research*, vol. 14, no. 4, article 802, 2012.

[39] A. G. Cullis, L. T. Canham, and P. D. J. Calcott, "The structural and luminescence properties of porous silicon," *Journal of Applied Physics*, vol. 82, no. 3, pp. 909–965, 1997.

[40] D. Kovalev, H. Heckler, G. Polisski, and F. Koch, "Optical properties of Si nanocrystals," *Physica Status Solidi (B)*, vol. 215, no. 2, pp. 871–932, 1999.

[41] M. Fujii, "Optical properties of intrinsic and shallow impurity-doped silicon nanocrystals," in *Silicon Nanocrystals: Fundamentals, Synthesis and Applications*, L. Pavesi and R. Turan, Eds., pp. 43–68, Wiley-VCH, Weinheim, Germany, 2010.

[42] J. Ma, S. H. Wei, N. R. Neale, and A. J. Nozik, "Effect of surface passivation on dopant distribution in Si quantum dots: the case of B and P doping," *Applied Physics Letters*, vol. 98, no. 17, Article ID 173103, 3 pages, 2011.

[43] C. Delerue, G. Allan, and M. Lannoo, "Theoretical aspects of the luminescence of porous silicon," *Physical Review B*, vol. 48, no. 15, pp. 11024–11036, 1993.

[44] M. Fujii, Y. Yamaguchi, Y. Takase, K. Ninomiya, and S. Hayashi, "Photoluminescence from impurity codoped and compensated Si nanocrystals," *Applied Physics Letters*, vol. 87, no. 21, Article ID 211919, 3 pages, 2005.

[45] D. V. Melnikov and J. R. Chelikowsky, "Quantum confinement in phosphorus-doped silicon nanocrystals," *Physical Review Letters*, vol. 92, no. 4, Article ID 046802, 4 pages, 2004.

[46] X. D. Pi, L. Mangolini, S. A. Campbell, and U. Kortshagen, "Room-temperature atmospheric oxidation of Si nanocrystals after HF etching," *Physical Review B*, vol. 75, no. 8, Article ID 085423, 5 pages, 2007.

[47] A. Gupta, M. T. Swihart, and H. Wiggers, "Luminescent colloidal dispersion of silicon quantum dots from microwave plasma synthesis: exploring the photoluminescence behavior across the visible spectrum," *Advanced Functional Materials*, vol. 19, no. 5, pp. 696–703, 2009.

[48] B. N. Jariwala, O. S. Dewey, P. Stradins, C. V. Ciobanu, and S. Agarwal, "In situ gas-phase hydrosilylation of plasma-synthesized silicon nanocrystals," *ACS Applied Materials and Interfaces*, vol. 3, no. 8, pp. 3033–3041, 2011.

[49] M. V. Wolkin, J. Jorne, P. M. Fauchet, G. Allan, and C. Delerue, "Electronic states and luminescence in porous silicon quantum dots: the role of oxygen," *Physical Review Letters*, vol. 82, no. 1, pp. 197–200, 1999.

[50] A. Puzder, A. J. Williamson, J. C. Grossman, and G. Galli, "Surface control of optical properties in silicon nanoclusters," *Journal of Chemical Physics*, vol. 117, no. 14, pp. 6721–6729, 2002.

[51] X. B. Chen, X. D. Pi, and D. Yang, "Bonding of oxygen at the oxide/nanocrystal interface of oxidized silicon nanocrystals: an ab initio study," *Journal of Physical Chemistry C*, vol. 114, no. 19, pp. 8774–8781, 2010.

[52] K. Seino, F. Bechstedt, and P. Kroll, "Influence of SiO_2 matrix on electronic and optical properties of Si nanocrystals," *Nanotechnology*, vol. 20, no. 13, Article ID 135702, 2009.

[53] M. Fukuda, M. Fujii, H. Sugimoto, K. Imakita, and S. Hayashi, "Surfactant-free solution-dispersible Si nanocrystals surface modification by impurity control," *Optics Letters*, vol. 36, no. 20, pp. 4026–4028, 2011.

[54] F. Erogbogbo, T. Liu, N. Ramadurai et al., "Creating ligand-free silicon germanium alloy nanocrystal inks," *ACS Nano*, vol. 5, no. 10, pp. 7950–7959, 2011.

[55] Z. C. Holman and U. R. Kortshagen, "Nanocrystal inks without ligands: stable colloids of bare germanium nanocrystals," *Nano Letters*, vol. 11, no. 5, pp. 2133–2136, 2011.